LIMNOLOGY
and
OCEANOGRAPHY

ASLO

Limnol. Oceanogr. 00, 2017, 00–00

doi: 10.1002/lno.10504

Delving deeper: Metabolic processes in the metalimnion of stratified lakes

Darren P. Giling,[1,a]* Peter A. Staehr,[2] Hans Peter Grossart,[1,3] Mikkel René Andersen,[4] Bertram Boehrer,[5] Carmelo Escot,[6] Fatih Evrendilek,[7] Lluís Gómez-Gener,[8] Mark Honti,[9] Ian D. Jones,[10] Nusret Karakaya,[7] Alo Laas,[11] Enrique Moreno-Ostos,[12] Karsten Rinke,[5] Ulrike Scharfenberger,[13,14] Silke R. Schmidt,[13,15] Michael Weber,[5] R. Iestyn Woolway,[16] Jacob A. Zwart,[17] Biel Obrador[8]

[1]Department of Experimental Limnology, Leibniz-Institute of Freshwater Ecology and Inland Fisheries (IGB), Stechlin, Germany
[2]Department of Bioscience, Aarhus University, Roskilde, Denmark
[3]Institute of Biochemistry and Biology, Potsdam University, Potsdam, Germany
[4]Freshwater Biological Laboratory, Faculty of Science, University of Copenhagen, Copenhagen, Denmark
[5]Department of Lake Research, Helmholtz-Centre for Environmental Research, Magdeburg, Germany
[6]Empresa Metropolitana de Abastecimiento y Saneamiento de Aguas de Sevilla, S.A. EMASESA., Sevilla, Spain
[7]Department of Environmental Engineering, Abant Izzet Baysal University, Bolu, Turkey
[8]Department of Evolutionary Biology, Ecology and Environmental Sciences, University of Barcelona, Barcelona, Spain
[9]MTA-BME Water Research Group, Hungarian Academy of Sciences, Budapest, Hungary
[10]Lake Ecosystems Group, Centre for Ecology & Hydrology, Lancaster Environment Centre, Bailrigg, Lancaster, UK
[11]Centre for Limnology, Estonian University of Life Sciences, Tartu, Estonia
[12]Department of Ecology, Marine Ecology and Limnology Research Group, University of Málaga, Málaga, Spain
[13]Department of Ecosystem Research, Leibniz-Institute of Freshwater Ecology and Inland Fisheries (IGB), Berlin, Germany
[14]Department of Biology, Chemistry and Pharmacy, Freie Universität Berlin, Berlin, Germany
[15]University of Potsdam, Institute of Earth and Environmental Sciences, Potsdam, Germany
[16]Department of Meteorology, University of Reading, Reading, UK
[17]Department of Biological Sciences, University of Notre Dame, Notre Dame, Indiana, USA

Abstract

Many lakes exhibit seasonal stratification, during which they develop strong thermal and chemical gradients. An expansion of depth-integrated monitoring programs has provided insight into the importance of organic carbon processing that occurs below the upper mixed layer. However, the chemical and physical drivers of metabolism and metabolic coupling remain unresolved, especially in the metalimnion. In this depth zone, sharp gradients in key resources such as light and temperature co-occur with dynamic physical conditions that influence metabolic processes directly and simultaneously hamper the accurate tracing of biological activity. We evaluated the drivers of metalimnetic metabolism and its associated uncertainty across 10 stratified lakes in Europe and North America. We hypothesized that the metalimnion would contribute highly to whole-lake functioning in clear oligotrophic lakes, and that metabolic rates would be highly variable in unstable polymictic lakes. Depth-integrated rates of gross primary production (GPP) and ecosystem respiration (ER) were modelled from diel dissolved oxygen curves using a Bayesian approach. Metabolic estimates were more uncertain below the epilimnion, but uncertainty was not consistently related to lake morphology or mixing regime. Metalimnetic rates exhibited high day-to-day variability in all trophic states, with the metalimnetic contribution to daily whole-lake GPP and ER ranging from 0% to 87% and $< 1\%$ to 92%, respectively. Nonetheless, the

*Correspondence: darren.giling@idiv.de

[a]Present address: German Centre for Integrative Biodiversity Research (iDiv) Halle-Jena-Leipzig, Leipzig, Germany; Institute of Biology, Leipzig University, Leipzig, Germany; Institute of Ecology, University of Jena, Jena, Germany

Additional Supporting Information may be found in the online version of this article.

metalimnion of low-nutrient lakes contributed strongly to whole-lake metabolism on average, driven by a collinear combination of highlight, low surface-water phosphorous concentration and high metalimnetic volume. Consequently, a single-sensor approach does not necessarily reflect whole-ecosystem carbon dynamics in stratified lakes.

Many lakes exhibit thermal stratification for a substantial portion of the year, developing marked vertical gradients in physical and chemical properties (Boehrer and Schultze 2008). These gradients influence biogeochemical processes such as organic and inorganic matter cycling (Coloso et al. 2008; Van de Bogert et al. 2012) and alter patterns of energy flow through lake food webs (Wilkinson et al. 2014). Consequently, patterns of stratification affect the important contribution that inland waters make to global carbon fluxes (Cole et al. 2007; Coloso et al. 2008; Staehr et al. 2012*b*). Vertical patterns of ecosystem metabolism vary among chemically and morphologically diverse lakes (Obrador et al. 2014), but information on the drivers of metabolism below the upper mixed layer (epilimnion) remains limited. However, a recent expansion of high-frequency and depth-integrated monitoring of lakes provides an opportunity to extend our understanding of lake metabolism into the metalimnion (Staehr et al. 2010; Obrador et al. 2014; Meinson et al. 2015).

Light availability is a key driver of gross primary production (GPP; for glossary see Table 1) below the upper mixed layer (Sadro et al. 2011*a*; Staehr et al. 2012*b*; Obrador et al. 2014). Light availability in the metalimnion is determined by two physical factors; the thickness of the epilimnion (Z_{mix}) and light attenuation in the epilimnion (K_D). These characteristics vary distinctly among lakes with different chemical characteristics, potentially exerting a strong control on biological processes in the metalimnion. Nutrient availability in surface waters controls phytoplankton biomass, so that trophic state and light availability in deeper layers are correlated. Planktonic communities below the epilimnion in eutrophic lakes may be shaded by high plankton densities in upper layers, while stratification reinforces nutrient limitation and thus the relative clarity of surface waters in oligotrophic lakes (Obrador et al. 2014). These physical and chemical influences on GPP indirectly affect other ecosystem functions. Metabolic coupling between GPP and ecosystem respiration (ER) is pronounced under oligotrophic conditions because heterotrophs are substrate limited and depend on labile photosynthetic exudates (Sadro et al. 2011*b*, 2014; Solomon et al. 2013).

In addition to distinct differences among lakes, day-to-day variation in ecosystem metabolism within lakes is substantial (Solomon et al. 2013). The magnitude of temporal variability differs among lakes, and may be related to physical processes determined by lake morphology and mixing regime (Solomon et al. 2013). For example, unstable and short-term stratification patterns could alter nutrient and organic matter (OM) fluxes among lake zones, affecting temporal and spatial patterns of metabolic activity. However, attributing biological activity at a specific place and time to physical processes in the metalimnion poses a considerable challenge (Coloso et al. 2011; Staehr et al. 2012*a*). Biological signals on diel timescales are dampened in the metalimnion, which is characterized by highly heterogeneous physical conditions. Therefore, hydrologic processes caused by external forcing (e.g., internal waves and advection; Boegman et al. 2003; Sadro et al. 2011*a*) need only be minor to contribute substantial noise to diel signals. Such processes alter the spatiotemporal footprint of sensors that measure the dissolved oxygen (DO) concentrations used in the estimation of ecosystem metabolism with the free-water method (Odum 1956). Thus, physical processes in the metalimnion may simultaneously influence metabolic processes and the ability to accurately estimate these metabolic processes using high-frequency DO measurements.

Understanding the chemical and physical drivers of metalimnetic metabolism and its uncertainty among diverse lake ecosystems would allow for a more accurate classification of stratified lakes as carbon sources or sinks. We investigated vertical patterns of lake metabolism, photosynthetic light-use efficiency, and the coupling relationship between ER and GPP using high-frequency and depth-specific data from 10 lakes and reservoirs that differed in nutrient concentration and thermal stratification patterns. We used a modelling technique that accounted for uncertainty in the estimation of metabolic parameters (following e.g., Hanson et al. 2008; Batt and Carpenter 2012; Cremona et al. 2014; Grace et al. 2015). This approach offers several advantages, including overcoming sources of error present in earlier "bookkeeping" methods (McNair et al. 2013) and allowing for the quantification of variation in diel DO that is not explained by the model. We assumed that unexplained variation in diel DO was predominantly attributable to process errors caused by lateral movements of water that are not incorporated in the depth-integrated framework.

We hypothesized that biological processes in the metalimnion are controlled primarily by light availability, which can be described by the ratio of the mixing depth (Z_{mix}) to the photic depth (Z_{eu}; determined by K_D) (Sadro et al. 2011*a*; Staehr et al. 2012*b*; Obrador et al. 2014). Thus, we expected that the contribution of the metalimnion to whole-lake metabolism would be highest in clear, oligotrophic lakes (i.e., low $Z_{mix} : Z_{eu}$). Day-to-day variability in metabolic rates was hypothesized to be most pronounced in polymictic lakes with dynamic thermal structure. Finally, we expected a tighter relation between GPP and ER in the photic zone, especially in oligotrophic lakes, and ER to be more reliant on recalcitrant OM

Table 1. Glossary of acronyms and terms.

Parameter or acronym	Description	Unit
OM	Organic matter	
GPP	Gross primary production at in situ temperature	mg O_2 L^{-1} d^{-1}
GPP_{20}	Gross primary production standardized to 20°C	mg O_2 L^{-1} d^{-1}
ER	Ecosystem respiration at in situ temperature	mg O_2 L^{-1} d^{-1}
ER_{20}	Ecosystem respiration standardized to 20°C	mg O_2 L^{-1} d^{-1}
Background respiration	Respiration of OM that was not recently or locally synthesized; the intercept of the correlation between ER_{20} and GPP_{20}	mg O_2 L^{-1} d^{-1}
NEP	Net ecosystem production (GPP-ER); describes whether the layer or lake is net autotrophic or net heterotrophic	mg O_2 L^{-1} d^{-1}
TP	Total phosphorous concentration	μg L^{-1}
TN	Total nitrogen concentration	μg L^{-1}
DO_{sat}	Dissolved oxygen concentration at atmospheric equilibrium	mg L^{-1}
DO_{mod}	Modeled dissolved oxygen concentration	mg L^{-1}
Z_{mix}	Mixing depth; bottom of the epilimnion and top of the metalimnion	m
Z_{eu}	Photic depth; equal to the depth with 1% of surface light	m
$Z_{mix} : Z_{eu}$	Ratio of mixing to photic depth. Describes light availability in the metalimnion	
T	Temperature	°C
DOC	Dissolved organic carbon	mg L^{-1}
Chl *a*	Chlorophyll-*a* concentration	μg L^{-1}
DCM	Deep chlorophyll maximum; algal layer in the meta- or hypolimnion	
PAR_0	Incoming photosynthetic active radiation at the water surface	μmol m^{-2} s^{-1}
PAR_z	Photosynthetic active radiation at depth z	μmol m^{-2} s^{-1}
K_D	Light attenuation coefficient	m^{-1}
U_{10}	Wind speed at 10 m above the surface of a lake	m s^{-1}
D_s	Atmospheric exchange	mg O_2 L^{-1} h^{-1}
K_s	Coefficient of gas exchange with the atmosphere	m h^{-1}
D_v	Vertical exchange between each layer and the adjacent layers due to turbulent diffusivity	mg O_2 L^{-1} h^{-1}
N^2	Brunt–Väisälä buoyancy frequency (local stability)	s^{-2}
K_v	Vertical eddy diffusivity coefficient	m^2 h^{-1}
D_z	Exchange due to mixed-layer deepening	mg O_2 L^{-1} h^{-1}
WLVW	Areal whole-lake volume-weighted estimate of metabolism (following Sadro et al. 2011*a*)	g O_2 m^{-2} d^{-1}
$Prop_{metab}$	Proportion of WLWV metabolism occurring in a certain depth zone	
$Prop_{vol}$	Proportion of whole lake volume occurring in a certain depth zone	
$Prop_{metab} : Prop_{vol}$	Ratio of the proportion metabolism to the proportion volume; ratio is > 1 when a depth zone contributes more metabolically than it does volumetrically	

under low-light conditions (Solomon et al. 2013; Obrador et al. 2014). We sought to identify the circumstances where depth-integrated estimates are required to accurately estimate whole-lake functioning by examining vertical patterns of metabolism across a diverse set of lakes.

Methods

Study sites

We modelled open-water lake metabolism from high-frequency, depth-specific measurements of DO and water temperature (T) in ten lakes and reservoirs across Europe and North America. The dataset included monomictic, dimictic, and polymictic lakes with a range of morphological characteristics and chemical composition (Table 2). Concentrations of nutrients, dissolved organic carbon (DOC) and chlorophyll *a* (Chl *a*) were determined from samples taken on 1–11 d at each lake during the stratified period (see Supporting Information Text 1 for sampling and analytical methods). In addition, Chl-*a* concentrations were obtained from high-frequency in situ measurements using a fluorometer at some

Table 2. Site information and ancillary data for the selected study lakes and reservoirs. Chemical and biological data are mean measurements from 1 to 11 samples taken during the period of stratification in each lake (Supporting Information Text 1). "Epi." denotes the epilimnion (metalimnion and hypolimnion measurements are presented in Supporting Information Table S1). The column "No. days" shows the total number of stratified days with metabolic estimates in each lake, with the number of days with at least one successful model fit in each depth zone (epi-, meta-, and hypolimnion) shown in the brackets.

Lake	Location	No. days	Trophic status	Mixing regime	Max. depth (lake) m	Max. depth (profile) m	Mean Z_{mix} m	Mean Z_{eu} m	Mean meta. thickness m	Epi. TP μg L^{-1}	Epi. TN μg L^{-1}	Epi. DOC μg L^{-1}	Epi. Chl *a* μg L^{-1}
Abant	Turkey	17 (2)	oligo.	mono.	18	12.75	5.6	11.9	2.6	14.0	1.5		1.5
Ontario	USA	69 (17)	oligo.	mono.	244	35	10.3	23.2	10.3	6.4			0.7
Stechlin	Germany	41 (32)	oligo.	di.	69.5	17.25	6.8	12.7	5.1	12.2	0.4	5.0	1.9
Rappbode pre-dam	Germany	48 (19)	meso.	di.	17	15.75	2.6	4.7	4.7	25.2	0.7	4.8	9.4
Bure	Denmark	58 (29)	meso.	poly.	11	9.5	4.3	7.5	3.3	22.9	0.7		5.5
Hampen	Denmark	56 (15)	meso.	poly.	13	9.5	4.4	6.3	3.1	23.6	0.6	3.0	8.7
El Gergal	Spain	21 (17)	meso.	mono.	37	19.75	5.3	6.5	6.1				24.1
Vedsted	Denmark	60 (14)	eu.	di.	11	9.5	3.5	4.0	3.8	27.3	0.5	4.9	41.4
Müggel	Germany	28 (17)	eu.	poly.	7.7	5.25	1.5	3.0	2.0	63.5	0.8	7.2	35.3
Castle	Denmark	32 (16)	hypereu.	poly.	9	8.5	4.4	2.3	2.6	94.1	1.6	3.4	46.3

sites. Data from each lake represented a single year, for a period ranging from several weeks to multiple months. Only days when the water-column was thermally stratified (as described below) were included in analyses (17–69 d per lake).

The profiling systems or sensor chains recorded high-frequency measurements (10–60 min intervals) at 3–35 depths in each lake, with at least one measurement point in each depth zone (i.e., the epi-, meta- and hypolimnion; Fig. 1; Supporting Information Table S1). Each measurement represented a horizontal layer of water centered on the measurement depth and having a thickness equal to the vertical resolution of measurements. Therefore, the deepest point of the profile was the depth of the deepest measurement plus half the vertical resolution of that layer. Meteorological data including photosynthetically active radiation (PAR), wind speed and barometric pressure were recorded at the same frequency as sub-surface measurements. Radiation measurements recorded as irradiance (E; W m^{-2}) were converted to photon flux in the 400–700 nm range (PAR; μmol m^{-2} s^{-1}) as follows (McCree 1981; Kirk 1994):

$$\mathrm{PAR} = E \times 4.6 \times 0.45. \quad (1)$$

Vertical stratification and underwater light regime

High vertical resolution (0.1 m) temperature profiles were modelled from available T data to determine whether a lake was stratified on a given day and to delineate the metalimnion. T at each depth z was modelled as (Rimmer et al. 2005):

$$T(z) = T_h + (T_e - T_h)\left(\frac{1}{1 + (\alpha \times z)^n}\right)^{1-\left(\frac{1}{n}\right)}, \quad (2)$$

where T_e and T_h are the maximum temperature in the epilimnion and hypolimnion, respectively, and α and n are model-estimated constants. Temperature curves were fitted in a Bayesian framework with JAGS (Plummer 2003) using normally distributed, maximum-entropy priors. The metalimnion extent (i.e., Z_{mix} to the top of the hypolimnion) was defined using water density ρ (kg L^{-1}), calculated as:

$$\rho = \rho_{max} - 6.63 \times 10^{-6}(T-4)^2. \quad (3)$$

The threshold gradient in density between adjacent points that defined Z_{mix} was selected by visual inspection for each lake individually (Supporting Information Fig. S1), and ranged between 0.03 kg m^{-3} m^{-1} and 0.18 kg m^{-3} m^{-1} (Read et al. 2011). The bottom of the metalimnion was similarly the deepest point with that density gradient. The sensitivity of metalimnetic volume and depth-zone metabolic rates to the selected density gradient threshold was examined at a subset of sites (Lake Ontario, Vedsted, and Müggel; see Supporting Information Text 2 and Supporting Information Table S2). The thermocline was defined as the depth with the highest density gradient (Read et al. 2011). Mean daily Z_{mix} and the bottom of the metalimnion were calculated as the mean of all profiles on each day, and each layer was assigned to one depth zone (i.e., epi-, meta-, or hypolimnion) for each day.

We calculated K_D at each site from either depth-integrated measurements of underwater PAR, Secchi depth or other existing site-specific relationships (Supporting Information Table S1). Estimates of K_D were made from daily to biweekly intervals and were linearly interpolated between measurement days when necessary. Where underwater PAR measurements were available, K_D was estimated as the slope of the

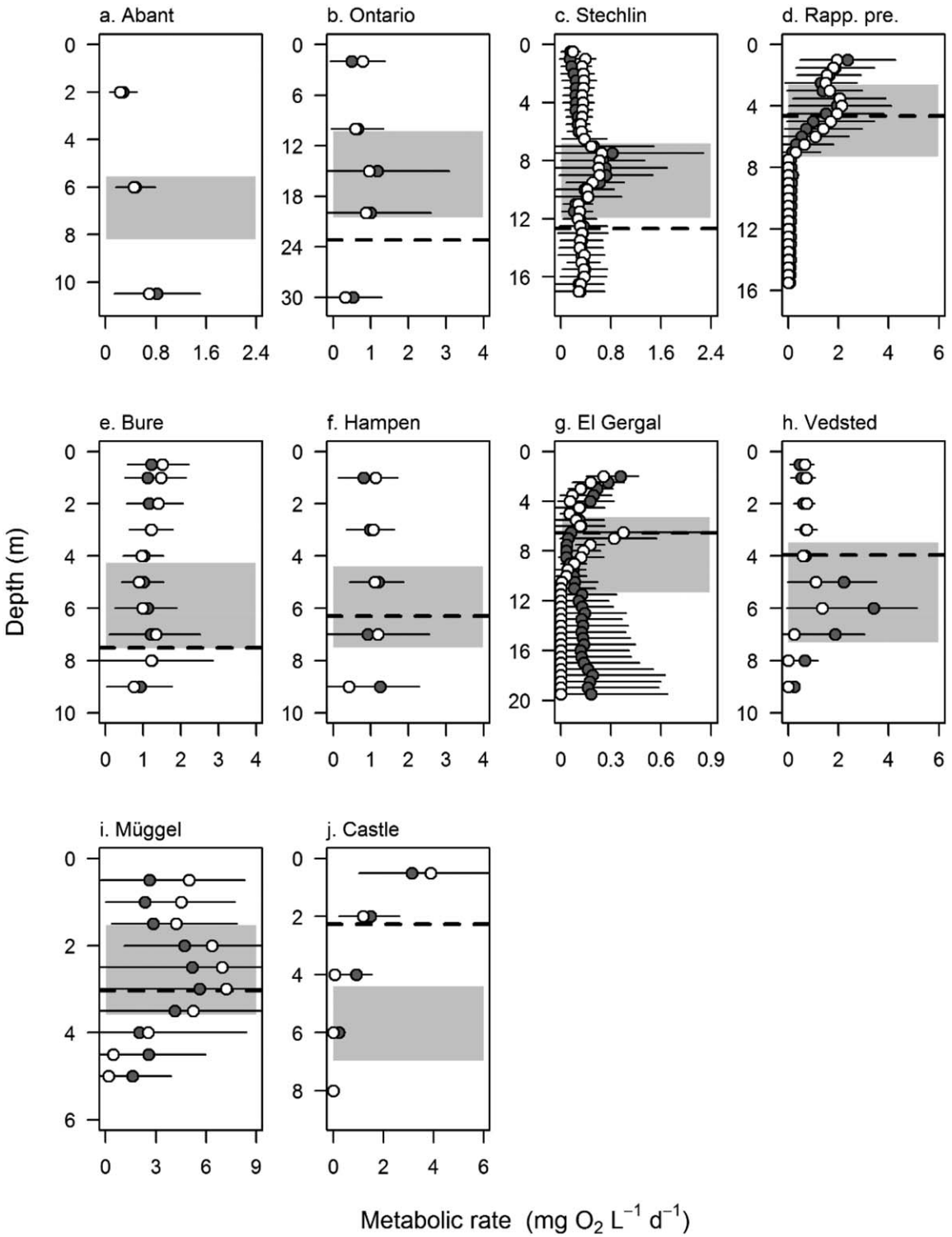

Fig. 1. Mean (± SD among days) depth-specific volumetric estimates of daily GPP (open white points) and ER (closed gray points) of adequately fit models over stratified days for each lake or reservoir: (**a**) Abant, (**b**) Ontario, (**c**) Stechlin, (**d**) Rappbode pre-dam, (**e**) Bure, (**f**) Hampen, (**g**) El Gergal, (**h**) Vedsted, (**i**) Müggel, and (**j**) Castle. The gray rectangle indicates the mean extent of the metalimnion and the dashed black line indicates the mean daily Z_{eu}.

linear regression between log(PAR) and depth z. Mean daily K_D was calculated from the K_D of each profile during daylight ($PAR_0 > 5$ μmol m^{-2} s^{-1}) that had a linear regression fit with $r^2 > 0.80$ (Staehr et al. 2012*b*; Obrador et al. 2014). Where Secchi depth was available, K_D was calculated as 1.7/Secchi depth (Poole and Atkins 1929). The mean daily photic depth (Z_{eu}) was calculated as $4.6/K_D$. Following the determination of daily K_D at each site, PAR for each time interval and depth z (PAR_z) was calculated from incident PAR (PAR_0) using the Beer–Lambert law:

$$PAR_z = PAR_0 \times e^{-K_D \times z}. \quad (4)$$

Model of depth-dependent metabolism

Gaps in the data series of up to 1 h were linearly interpolated before we applied a 4-h simple moving average smoothing to DO, PAR and wind speed measurements (following Obrador et al. 2014). To estimate mean daily rates of ecosystem metabolism, we used a Bayesian model with non-linear sub-models for GPP and ER (Giling et al. 2016). Changes in DO concentration between successive measurement times t for each layer were partitioned into the contribution by biotic and physical processes using a depth-specific diel oxygen model (Staehr et al. 2012*b*):

$$DO(t+1) = DO(t) + NEP(t) - D_s(t) - D_v(t) + D_z(t); \quad (5)$$

where NEP is the rate of net ecosystem production for that timestep (mg O_2 L^{-1} t^{-1}), D_s is air-water exchange, D_v is diffusive vertical exchange between adjacent layers and D_z is metalimnetic exchange due to mixed-layer deepening. Atmospheric exchange (D_s) was applied only to layers in the epilimnion, and calculated as:

$$D_s(t) = K_s(t) \frac{DO_{mod}(t) - DO_{sat}(t)}{Z_{mix}(t)}. \quad (6)$$

The gas transfer velocity (K_s) was calculated at a Schmidt number of 600 (K_{600}) from wind speed standardized to 10 m height (U_{10}) according to Cole and Caraco (1998). In Eq. 6, DO_{mod} is the modelled DO concentration following Song et al. (2016) and DO_{sat} is DO concentration at atmospheric equilibrium (calculated from temperature and barometric pressure; Benson and Krause 1984). Vertical exchange between each layer and the adjacent layers due to turbulent diffusivity (D_v) was estimated using the Brunt–Väisälä buoyancy frequency (N^2 [s^{-2}], a measure of local stability; Boehrer and Schultze 2010) to calculate the vertical eddy diffusivity coefficient (K_v) according to Hondzo and Stefan (1993). Lake Ontario was an exception due to its surface area exceeding the applicable range of the model presented by Hondzo and Stefan (1993). The metalimnetic K_v for Lake Ontario was set as 6×10^{-6} m^2 s^{-1} based on measurements and theoretical work from Lakes Ontario and Erie (Sweers 1970; Bouffard et al. 2014). Epilimnetic and hypolimnetic K_v were expected to be higher than the metalimnetic estimate, so epi- and hypolimnetic K_v estimates at Lake Ontario were set using a factor determined from the average relative difference between depth zones in the other nine lakes. The influence of K_v estimates on metabolic rates at Ontario and two other lakes (Vedsted and Müggel) was assessed with a sensitivity analysis (for details see Supporting Information Text 2 and Supporting Information Table S2). The flux D_z was calculated as proportional to the Z_{mix} deepening rate ($\Delta Z_{mix}/\Delta t$) and was applied to measurement points within the metalimnion and 1 m above or below (Obrador et al. 2014). At some sites, we set a threshold limiting the deepening rate to a maximum of 5 m h^{-1} to prevent short-term surface-water microstratification inaccurately affecting D_z in the metalimnion. For a full description of the model see Staehr et al. (2012*b*).

Sub-models for the production and respiration components of NEP in Eq. 5 were parameterized according to Grace et al. (2015). For each layer, GPP was modelled as a saturation function of PAR_z, while respiration was non-linearly dependent on T at time t ($T(t)$):

$$NEP(t) = A \times PAR_z(t)^p - R_{\bar{T}} \left(\theta^{\left(T(t) - \bar{T}\right)} \right); \quad (7)$$

where the first component describes GPP per timestep (mg O_2 L^{-1} t^{-1}), and A is a parameter indicating primary production per unit light (i.e., photosynthetic efficiency), $PAR_z(t)$ is the depth-specific PAR at time t, and p is an estimated exponent that represents the ability of producers to use light and accounts for saturating photosynthesis (when $p < 1$). The second component indicates DO consumption by ER (mg O_2 L^{-1} t^{-1}); $R_{\bar{T}}$ is the respiration rate at $\bar{T}$, Θ describes the temperature dependence of respiration (set to 1.072, corresponding to Q_{10} of 2; Wilcock et al. 1998), T is the water temperature at time t and $\bar{T}$ is the mean daily temperature in that layer. Respiration was estimated at $\bar{T}$ rather than a standardized temperature because we were interested in vertical patterns among the lakes at in situ conditions. Modelled rates were standardized to a temperature of 20°C (GPP_{20} and ER_{20}; for results see Supporting Information Fig. S2) for analysing coupling between respiration and primary production (Holtgrieve et al. 2010; Solomon et al. 2013). We estimated the parameters A, p and $R_{\bar{T}}$ in Eq. 7 for each layer with a Bayesian approach in JAGS (Plummer 2003) using R code (R Development Core Team 2014) modified from Grace et al. (2015) following the rationale of Song et al. (2016). Prior distributions for the estimated parameters were uniformly distributed within known physical constraints as described by Grace et al. (2015). Mean daily metabolic estimates (and their propagated uncertainty) for each layer were calculated from estimated parameters as:

$$GPP = \sum_{t=1}^{\text{measurements}} A \times PAR(t)^p \quad (8)$$

$$ER = 86400 \times \frac{R_{\bar{T}}}{\Delta t} \quad (9)$$

where GPP is daily gross primary production (mg O_2 L^{-1} d^{-1}), ER is daily ecosystem respiration at daily average temperature (mg O_2 L^{-1} d^{-1}) and 86,400 converts from seconds to days. Convergence and stationarity of Markov Chain Monte Carlo (MCMC) values were assessed with the Gelman-Rubin convergence statistic $\hat{R}$ (Brooks and Gelman 1997). Models with $\hat{R} > 1.1$ (indicating unconverged chains) as well as poor fitting models ($R^2 < 0.40$) were excluded from further analyses. Excluding poor fitting models did not substantially alter vertical patterns of ecosystem metabolism or their uncertainty (Supporting Information Fig. S3). Example model fits for each lake are available in the supplementary material (Supporting Information Figs. S7–S16) and example code for estimating depth-integrated metabolic rates is available online (github.com/dgiling).

Aggregating layer-specific metabolic rates

Mean daily rates in each depth zone (i.e., the epi-, meta-, and hypolimnion) were calculated as the mean of all layers assigned to that depth zone on that day. The standard deviation of the aggregated depth-zone rate (σ_{zone}) was propagated from the modelled uncertainties in each layer i as follows:

$$\sigma_{\text{zone}} = \sqrt{\sum_{i}^{no.\ layers} \sigma_i^2}, \quad (10)$$

where i to *no. layers* are the layers belonging to that depth zone. The aggregated depth-zone estimates were used for further analysis of metabolic rates. Due to high day-to-day variability, only days when there was at least one adequate metabolic model fit (i.e., $\hat{R} < 1.1$ and $R^2 > 0.40$) from layers in each depth zone were considered to calculate the contribution of the metalimnion to whole-lake metabolism (total of 178 d; Table 2).

Whole-lake metabolism estimates

Whole-lake volume-weighted estimates (WLVW; Sadro et al. 2011*a*) were calculated by multiplying the daily depth-zone volumetric rates (in g O_2 L^{-1} d^{-1}) by the total volume of each depth zone (L zone water) before summing the three zones and dividing by the sum of the zone volumes (L lake water). Metalimnetic volume was calculated using surface areas from hypsographic data and mean daily thickness from high-resolution temperature profiles. Whole-lake areal rates (g O_2 m^{-2} d^{-1}) were obtained by dividing the WLWV estimate by the lake surface area (m^2). Hypolimnetic volume and thus metabolic contribution will be underestimated in the small number of lakes that were considerably deeper than the available profile measurements (e.g., Lake Ontario; Table 2). The proportional contribution of the metalimnion to whole-lake metabolism was calculated as the metalimnetic volumetric rate divided by the WLVW estimate (termed "$\text{Prop}_{\text{metab}}$"). We also assessed whether the metalimnion disproportionately contributed to whole-lake metabolic activity for its size (volume). We did this by calculating the ratio between $\text{Prop}_{\text{metab}}$ and the metalimnetic contribution to whole-lake volume (termed "Prop_{vol}"). Thus, the metalimnion contributed more to the whole lake metabolically than it did volumetrically when the ratio $\text{Prop}_{\text{metab}} : \text{Prop}_{\text{vol}}$ was > 1.

We assessed how traditional metabolism estimates based on single sensors in the epilimnion compared to depth-integrated estimates. "Single-sensor estimates" were calculated by taking the sensor placed at 1 m depth, the most widespread DO sensor deployment depth (Solomon et al. 2013), and calculating whole-lake areal metabolism as above assuming that this rate was constant over depth. The shallowest available probe (either 0.5 m or 2 m) was used when no sensor was available at 1 m depth.

The "background respiration" of OM can be inferred from the intercept of the relationship between daily ER_{20} and daily GPP_{20}, i.e., ER_{20} when $GPP_{20} = 0$ (del Giorgio and Williams 2005; Solomon et al. 2013). The slope of the relationship between daily ER_{20} and GPP_{20} describes the metabolic coupling, where a slope of 1 indicates a unit increase in ER_{20} for each unit increase in GPP_{20}. The coefficient of determination (r^2) indicates the strength of the coupling (Obrador et al. 2014). We used estimates from layers where there were > 5 d with successful fits to estimate coupling regression parameters. Models were excluded when the layer was nearly always dark (so that GPP_{20} was zero or mean < 0.01 mg O_2 L^{-1} d^{-1}) because the slope was either vertical (and therefore undefined) or highly outlying (20–40 times the mean slope) and not conceptually meaningful. Coupling estimates for depth zones were calculated as the mean of all intercept and slope estimates from layers belonging to that depth zone.

Statistical analyses

Comparisons among depth zones, correlations with ancillary variables, and ER_{20}-GPP_{20} regressions were analyzed by fitting linear models or linear mixed models (LMMs) in R (R Development Core Team 2014). The LMMs included a random effect for site and layer and AR1 autocorrelation structure (nested within site) to account for repeated daily measurements where appropriate. We compared a range of autocorrelation structures (including AR2 and AR3) with Akaike Information Criterion (AIC) values and found AR1 provided equivalent or better support for the models. In LMMs, reported coefficients of determination (R^2) values refer to the variation explained by the fixed effects only. Variables were log-transformed when necessary. When there was collinearity among predictor variables we used principal components analysis (PCA) for variable reduction. The resulting principal components were subsequently used as explanatory variables in LMMs.

Results

Model validation and the importance of physical fluxes

The depth-integrated metabolic model provided a better description of diurnal changes in DO in the epilimnion (74% of models converged with adequate fit) than in the

metalimnion (43%) or hypolimnion (32%; Fig. 2a). Furthermore, modelled metabolic estimates were on average more precise in the epilimnion (mean coefficient of variation [CV] for GPP and ER estimates = 0.14 and 0.23, respectively) than in the metalimnion (mean GPP and ER CV = 0.25 and 0.33, respectively) or hypolimnion (mean GPP and ER CV = 0.35 and 0.51, respectively) (Fig. 2b,c). There was high variability in model fit (R^2) and estimate certainty (CV) among days and depth zones (Fig. 2). In the metalimnion, this variation was not well explained by local water-column stability, lake area, or the frequency and spatial resolution of measurements (see Supporting Information Text 3; Supporting Information Figs. S4 and S5).

The physical fluxes of DO (i.e., D_s, D_v, and D_z) contributed a substantial proportion (32% ± 24% across all estimates) of the total DO fluxes (i.e., sum of absolute NEP, D_s, D_v, and D_z) (Supporting Information Table S3). In the epilimnion, a mean of 45% of DO changes were attributable to the diffusive components, which was mostly atmospheric exchange (D_s) with a small contribution from D_v and D_z. Transfer due to mixed layer deepening (D_z) contributed strongly in the metalimnion (mean 29% attributable to diffusive fluxes), and both D_z and D_v estimates were important in the hypolimnion (combined mean 16%). The average magnitude of physical fluxes was unrelated to either the mean model R^2 ($F_{1,8} = 1.216$, $p = 0.302$) or the CV of GPP and ER estimates ($F_{1,8} = 3.499$, $p = 0.098$ and $F_{1,8} = 2.727$, $p = 0.173$) among the 10 lakes. Furthermore, physical processes were not strongly correlated with lake morphology in our dataset. In the metalimnion, log-transformed lake area did not affect the balance between total physical fluxes and NEP with ($F_{1,8} = 1.218$, $p = 0.301$) or without ($F_{1,7} = 1.892$, $p = 0.211$) outlying Lake Ontario (Supporting Information Fig. S5). Sensitivity analysis demonstrated that the magnitude of K_v did not strongly affect metabolic estimates, except for rates in the metalimnion and hypolimnion of polymictic Lake Müggel (Supporting Information Text 2 and Supporting Information Table S2).

Depth-specific metabolic rates and photosynthetic efficiency

Vertical patterns of metabolism varied distinctly among the lakes, with mean GPP ranging from 0.00 to 5.98 mg O_2 L^{-1} d^{-1} and ER from 0.00 to 3.74 mg O_2 L^{-1} d^{-1} across all depth zones (Fig. 1; Supporting Information Table S3). Surface layers were most often autotrophic, while balanced to net heterotrophic conditions were prevalent in the metalimnion. Mean NEP was negative for 60% of the daily metalimnetic estimates across all the lakes and layers. Mean daily GPP in the epilimnion was positively correlated with mean epilimnetic TP concentration ($F_{1,7} = 8.75$, $p = 0.021$, $r^2 = 0.56$), as was epilimnetic ER ($F_{1,7} = 10.59$, $p = 0.014$, $r^2 = 0.60$). In the metalimnion, mean GPP and ER were not linearly correlated to epilimnetic TP concentration ($F_{1,7} = 2.04$, $p = 0.196$, $r^2 = 0.22$ and $F_{1,7} = 0.10$, $p = 0.404$, $r^2 = 0.10$, respectively; Fig. 3a,b).

We found evidence of photosynthetic activity down to ca. 0.1% of surface light. Increasing GPP with depth in some lakes was due to higher photosynthetic efficiency (i.e., parameter A from Eq. 7; GPP [mg O_2 L^{-1} d^{-1}]/PAR [μmol m^{-2} s^{-1}]) in lower light conditions ($F_{1,792} = 105.17$, $p < 0.001$; Supporting Information Fig. S6). Correspondingly, photosynthetic efficiency varied by depth zone ($F_{2,809} = 58.55$, $p < 0.001$). Photosynthetic efficiency was lower in the epilimnion than in the metalimnion or hypolimnion ($p < 0.01$ in post-hoc pairwise comparisons), while the meta- and hypolimnetic photosynthetic efficiency did not differ ($p = 0.905$). Photosynthetic efficiency was reduced in low nutrient conditions ($F_{2,23} = 25.72$, $p < 0.001$). Thus efficiency was significantly lower in oligotrophic lakes than in mesotrophic lakes (post-hoc comparison; $z = -4.54$, $p < 0.001$), which were lower again than eutrophic lakes ($z = -3.17$, $p = 0.004$).

Temporal variability in metabolic rates

Metabolic estimates were characterized by high day-to-day variability in some lakes and layers (Fig. 1). For contiguous days with adequate model fits, between 8–52%, 0–78%, and 11–100% of epi-, meta-, and hypolimnetic GPP estimates among the 10 lakes were within 2 standard deviations (SD) of the estimate from the previous day. Similarly, between 13–53%, 0–88%, and 11–96% of epi-, meta- and hypolimnetic ER estimates were within 2 SD of the previous days' estimate. In the metalimnion, this variability did not appear to be strongly driven by PAR; the day-to-day shift in PAR_z did not consistently differ between consecutive days that had similar or disparate metabolic estimates. The proportion of days with estimates similar to the previous day was also not related to lake area (Supporting Information Fig. S5). Day-to-day variability in metalimnetic thickness (relative to Z_{max}) was slightly higher in polymictic (SD in relative thickness = 0.08 ± 0.02, $n = 4$ lakes) than in mono-/dimictic lakes (SD = 0.04 ± 0.02, $n = 6$ lakes, $F_{1,8} = 6.33$, $p = 0.04$). However, metalimnetic local water-column stability did not differ among mixing regimes ($F_{1,8} = 3.26$, $p = 0.109$). Variability among daily estimates of GPP and ER in the metalimnion (Supporting Information Table S3) was not related to lake mixing regime ($F_{2,7} = 0.753$, $p = 0.505$ and $F_{2,7} = 0.044$, $p = 0.957$) or trophic status ($F_{2,7} = 1.337$, $p = 0.223$ and $F_{2,7} = 0.178$, $p = 0.841$). We assessed whether process errors (e.g., lateral water movements) were a driver of temporal variation in metabolic estimates by testing whether among-day SD in metabolic rates was higher when depth-zone means were aggregated from models with adequate ($R^2 > 0.4$) or poor fits ($R^2 < 0.4$). Model fit did not influence temporal variation in metalimnetic GPP (paired t-test; $t_9 = 1.42$, $p = 0.190$) or ER ($t_9 = 0.772$, $p = 0.460$).

Metalimnetic contribution to whole-lake metabolism

Across all sites, the proportional contribution of the metalimnion to WLVW metabolic estimates (i.e., $Prop_{metab}$)

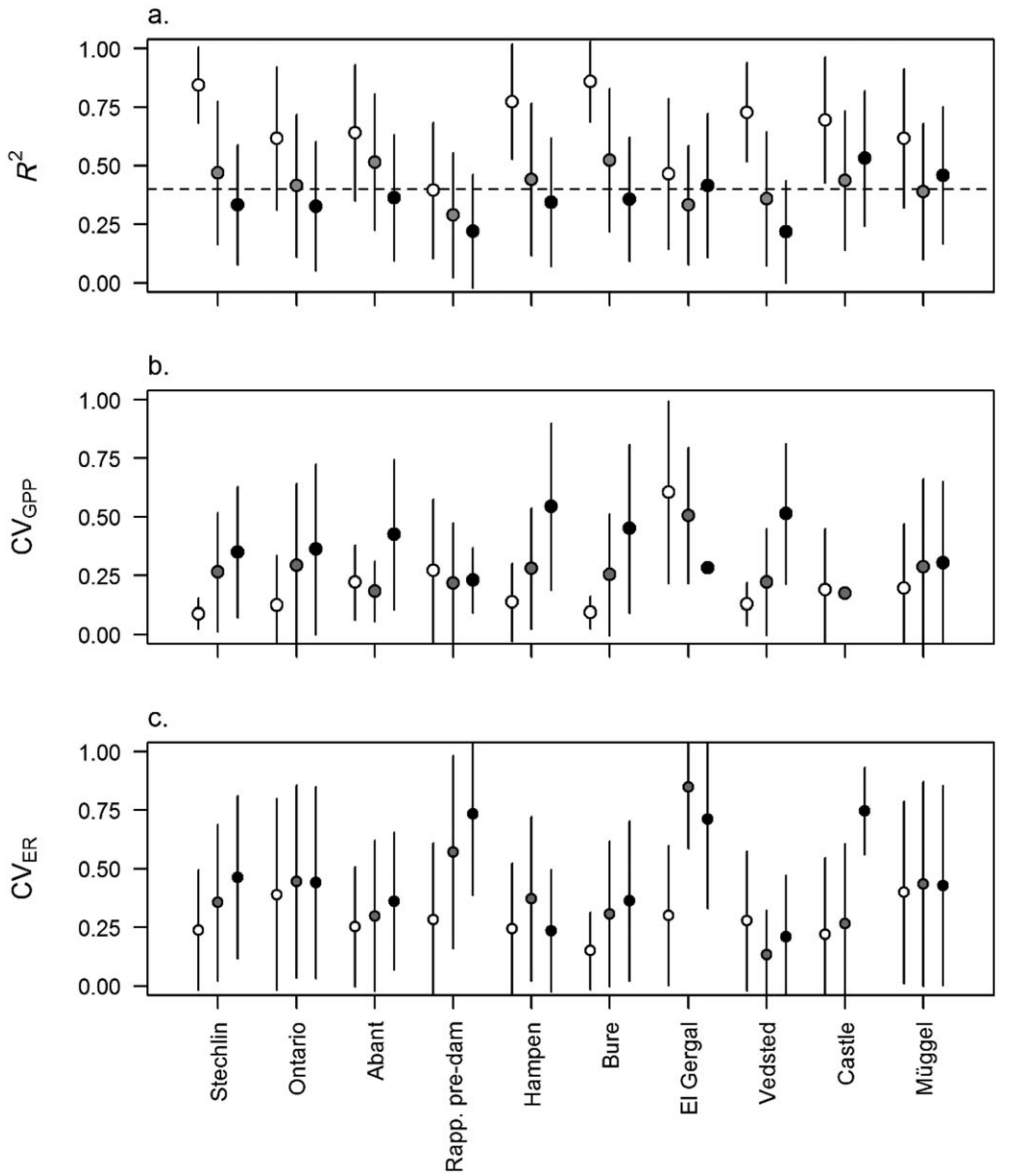

Fig. 2. Mean (± SD) (**a**) R^2, (**b**) coefficient of variation (CV) of GPP estimates, and (**c**) CV of ER estimates from all models across the study lakes and depth zones. White, gray, and black points show epi-, meta-, and hypolimnetic zones, respectively. Values above the dashed horizontal line at $R^2 = 0.40$ in panel (**a**) were considered to have adequate model fit.

varied between 0% and 87% for daily GPP and between < 1% and 92% for daily ER. The metalimnetic $Prop_{metab}$ was negatively correlated to epilimnetic TP concentration for GPP ($F_{1,7} = 6.09$, $p = 0.042$, $r^2 = 0.47$) and for ER ($F_{1,7} = 8.69$, $p = 0.021$, $r^2 = 0.55$), but these relationships were driven by Castle Lake (Fig. 3c,d) and were not robust to its exclusion. The contribution of the metalimnion to whole-lake volume (i.e., $Prop_{vol}$) was between 3% and 60% (mean 32%). The metalimnetic $Prop_{metab}$ was positively correlated with metalimnetic $Prop_{vol}$ for both GPP (slope = 0.88 ± 0.12, $F_{1,175} = 58.46$, $p < 0.001$, $r^2 = 0.25$) and ER (slope = 0.94 ± 0.14, $F_{1,175} = 43.74$, $p < 0.001$, $r^2 = 0.20$). The metalimnetic $Prop_{metab}$: $Prop_{vol}$ was a mean 0.95 ± 0.67 SD for GPP and 1.06 ± 0.87 SD for ER. The ratio $Prop_{metab}$: $Prop_{vol}$ showed that the metalimnion disproportionately contributed metabolic activity for its volume (i.e., $Prop_{metab}$: $Prop_{vol} > 1$) in oligotrophic lakes (Fig. 3e,f). This was supported by a negative relationship between metalimnetic $Prop_{metab}$: $Prop_{vol}$ and mean epilimnetic TP concentration for GPP ($F_{1,7} = 15.31$, $p = 0.006$, $r^2 = 0.68$; Fig. 3e) and ER ($F_{1,7} = 12.46$, $p = 0.010$, $r^2 = 0.64$; Fig. 3f).

We observed a negative linear correlation between metalimnetic $Prop_{metab}$ and log-transformed Z_{mix} : Z_{eu} for GPP ($F_{1,166} = 12.39$, $p < 0.001$; Fig. 4a). However, this trend was

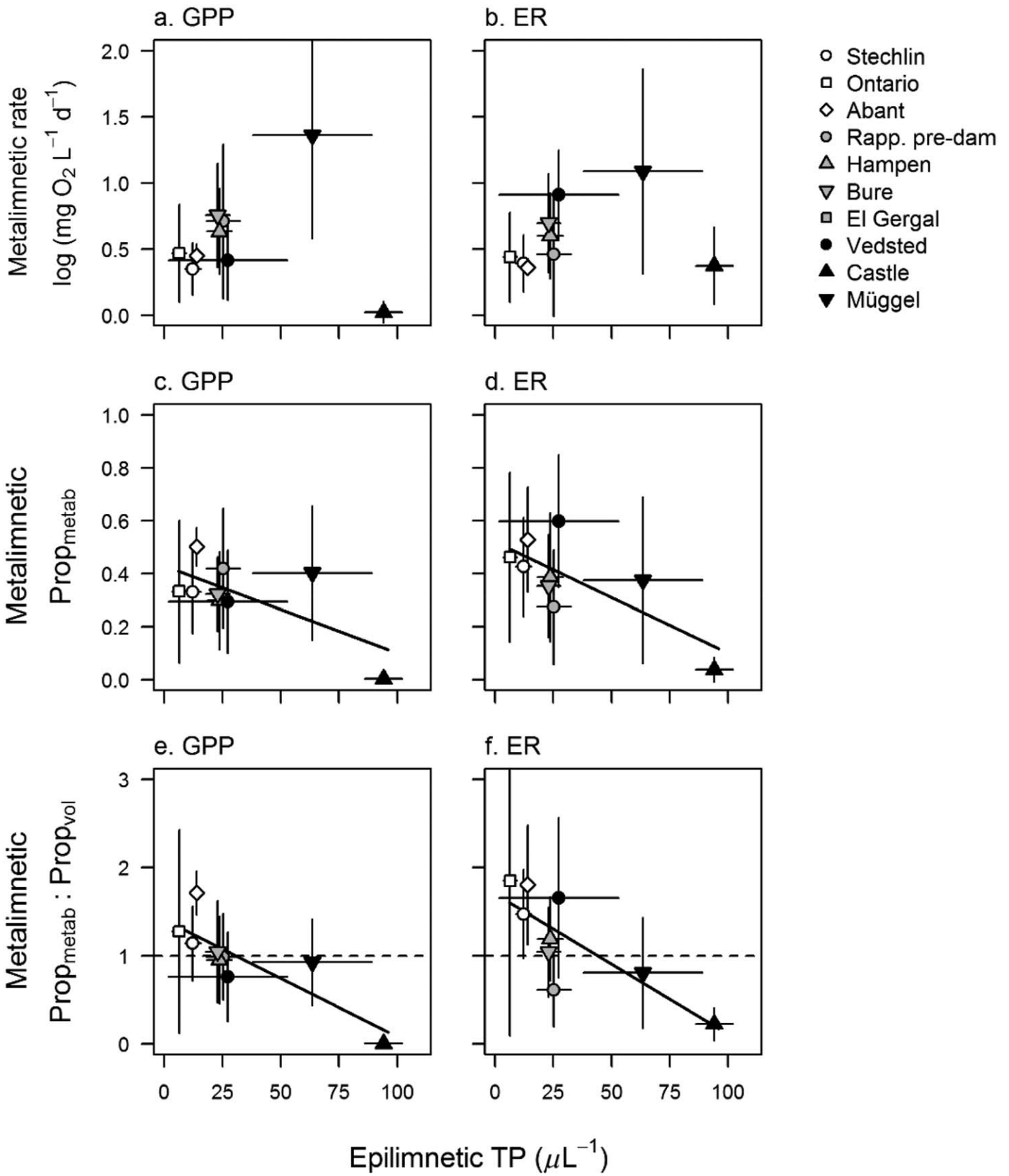

Fig. 3. Scatterplots showing the correlation between mean (± SD) epilimnetic total phosphorus (TP) and metalimnetic GPP (left) and ER (right). Plots show mean (± SD) metalimnetic volumetric rates (**a**, **b**), mean contribution of the metalimnion to whole lake metabolism ($Prop_{metab}$; **c**, **d**); and the ratio between $Prop_{metab}$ and the contribution of the metalimnion volume to whole-lake volume ($Prop_{metab}$: $Prop_{vol}$; **e**, **f**). Solid black lines indicate significant linear relationships in linear mixed models. White, gray, and black points indicate oligotrophic, mesotrophic, and eutrophic lakes, respectively. Circles, squares/diamonds, and triangles represent monomictic, dimictic, and polymictic lakes, respectively.

not robust to the exclusion of Castle Lake ($F_{1,151} = 2.47$, $p = 0.118$). A similar negative relationship was observed for metalimnetic ER $Prop_{metab}$ (Fig. 4b), with ($F_{1,166} = 18.58$, $p < 0.001$) or without ($F_{1,151} = 12.10$, $p < 0.001$) Castle Lake. Comparable trends were observed for the effect of log-transformed $Z_{mix} : Z_{eu}$ on $Prop_{metab} : Prop_{vol}$, with a negative relationship for GPP ($F_{1,166} = 15.22$, $p < 0.001$; Fig. 4c), which was again not significant when Castle Lake was omitted from the analysis ($F_{1,151} = 2.08$, $p = 0.151$). In contrast, the negative effect of log-transformed $Z_{mix} : Z_{eu}$ on $Prop_{metab} : Prop_{vol}$ for ER ($F_{1,166} = 12.46$, $p < 0.001$; Fig. 4d) was robust to the exclusion of Castle Lake ($F_{1,151} = 8.31$, $p = 0.005$). Metalimnetic $Prop_{vol}$ tended to be high when Z_{mix} was shallow, meaning that log $Z_{mix} : Z_{eu}$ and $Prop_{vol}$ were negatively correlated ($F_{1,166} = 13.20$, $p < 0.001$, $r^2 = 0.11$). Hence, we used PCA to examine the collinear drivers of metalimnetic $Prop_{metab}$. Principal components (PCs) were derived from four variables representing abiotic resource availability and physical conditions (PAR_z, temperature, $Prop_{vol}$, and N^2). The PC explaining the majority of variation (PC1) did not reduce the collinearity, as it was characterized by lower temperature, $Prop_{vol}$, and N^2 (Table 3). Metalimnetic $Prop_{metab}$ for GPP and ER was negatively correlated to PC1 in linear mixed models (Table 3), suggesting a combined importance of these factors. A second component (PC2) was characterized mainly by low PAR_z and high local stability N^2 in the metalimnion, and was negatively correlated with $Prop_{metab}$ for GPP and ER (Table 3).

Depth-specific metabolic coupling

Coupling between ER_{20} and GPP_{20} varied among the lakes and depth zones. Background respiration (intercept) ranged from −0.16 to 2.70 mg O_2 L^{-1} d^{-1}, mean coupling slope ranged from −0.07 to 1.26 and mean r^2 varied between 0.05 and 0.94 (Supporting Information Table S4). There was an interaction between the effect of depth zone and epilimnetic TP concentration on mean background respiration ($F_{2,17} = 7.19$, $p = 0.005$). Mean epilimnetic TP did not affect mean background respiration in the epilimnion ($F_{1,7} = 4.64$, $p = 0.068$; Fig. 5a), but there was a positive linear correlation in both the metalimnion ($F_{1,7} = 26.21$, $p = 0.002$; Fig. 5b) and hypolimnion ($F_{1,7} = 19.19$, $p = 0.012$; Fig. 5c). However, the positive relationship in the hypolimnion was driven predominantly by Lake Müggel, which is shallow and does not develop a hypolimnion that is stable over time. Across all TP levels, background respiration did not differ among depth zones ($F_{2,22} = 1.13$, $p = 0.340$). There was no interaction between the effect of epilimnetic TP and depth zone on the coupling slope ($F_{2,17} = 1.20$, $p = 0.324$), and no significant difference among depth zones ($F_{2,17} = 0.44$, $p = 0.653$). Across all depth zones, the coupling slope decreased with increasing epilimnetic TP concentration ($F_{1,17} = 6.48$, $p = 0.021$), but this relationship was not evident in any one depth zone individually ($p > 0.117$; Fig. 5d–f). For the strength of the coupling relationship (r^2) there was also no interaction between the effect of depth zone and mean epilimnetic TP ($F_{2,17} = 0.885$, $p = 0.431$), and no effect of depth zone ($F_{2,17} = 0.023$, $p = 0.977$). The strength of the coupling relationship decreased with increasing TP concentration ($F_{1,17} = 7.97$, $p = 0.012$) across all depth zones combined (Fig. 5g–i).

Effect of depth-integration on whole-lake areal estimates

We assessed how areal WLWV estimates of GPP, ER, and NEP made from a single epilimnetic sensor compared to the depth-integrated estimates. For mean GPP, the single-sensor approach over-estimated whole-lake metabolism at 9 of 10 lakes, but the average difference from integrated estimates varied across lakes (mean difference 3.17 ± 4.58 g O_2 m^{-2} d^{-1}; Fig. 6a). In contrast, single-sensor estimates of ER did not consistently vary from integrated estimates (mean difference -0.37 ± 3.40 g O_2 m^{-2} d^{-1}; Fig. 6b). Correspondingly, single-sensor estimates of whole-lake NEP generally were slight overestimates, but there was high variation both among lakes and among days within lakes (mean difference 3.55 ± 6.65 g O_2 m^{-2} d^{-1}; Fig. 6c).

Discussion

We found contrasting vertical patterns of metabolic rates among the stratified lakes (Fig. 1). In clearer lakes, mean daily rates of GPP and ER were weakly associated with depth (e.g., Lake Bure) or peaked in the metalimnion (e.g., Lakes Ontario and Stechlin), as reported previously (Sadro et al. 2011*a*). In contrast, the metabolic rates of some mesotrophic and eutrophic lakes were strongly depth-dependent (e.g., Castle Lake). In such cases, single-sensor estimates of whole-lake metabolism can potentially deviate considerably from depth-integrated estimates (Fig. 6). We found that the metalimnion can contribute substantially to daily whole-lake metabolism across a broad range of lakes (mean 29–50% of GPP and 27–60% of ER), with the exception of highly eutrophic conditions (Figs. 3, 4). However, the relative contribution of the metalimnion varied substantially among days regardless of lake stratification pattern, and metalimnetic $Prop_{metab}$ was only moderately explained by changes in light availability (as indicated by $Z_{mix} : Z_{eu}$). Nonetheless, on average the metalimnion of oligotrophic lakes contributed disproportionately to whole-lake metabolism for its volume ($Prop_{metab} : Prop_{vol} > 1$; Fig. 3e,f).

Importance of physical processes to model uncertainty and day-to-day variability

Our depth-integrated analysis extends current understanding of the role that physical processes play in obtaining accurate metabolic estimates (Van de Bogert et al. 2007; Coloso et al. 2008; Staehr et al. 2012*b*; Rose et al. 2014). We expected that high variability in patterns of stratification and low water-column stability would be associated with poor fitting models and high uncertainty in parameter

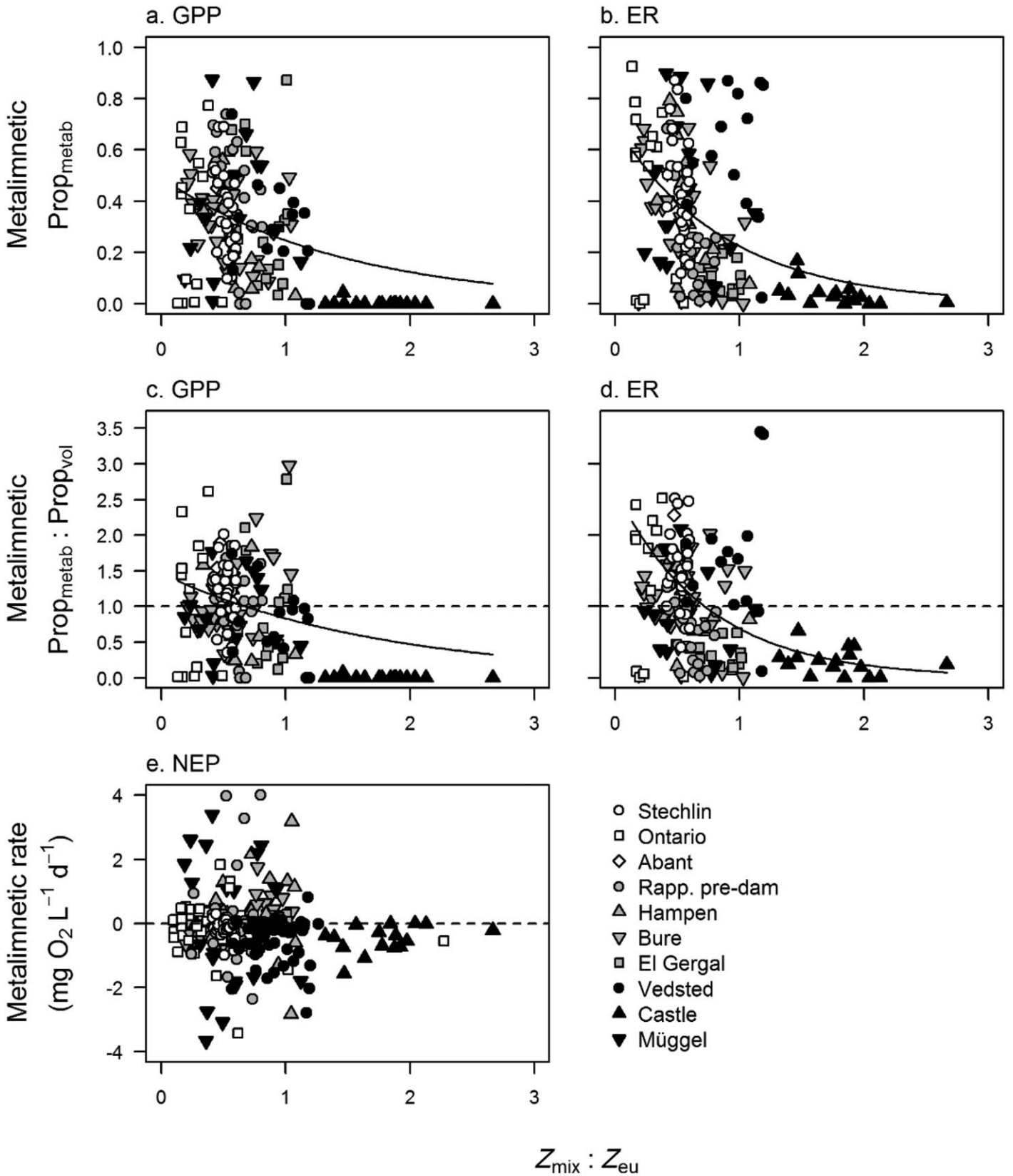

Fig. 4. Scatterplots showing the correlation between Z_{mix} : Z_{eu} and metalimnetic metabolism. The top row shows the proportional contribution of the metalimnion to whole-lake metabolism ($Prop_{metab}$) for (**a**) GPP and (**b**) ER. The middle row shows the effect of Z_{mix} : Z_{eu} on the ratio between $Prop_{metab}$ and the proportional contribution of the metalimnetic volume to whole-lake volume ($Prop_{metab}$: $Prop_{vol}$) for (**c**) GPP and (**d**) ER. At values higher than the dashed horizontal line at $Prop_{metab}$: $Prop_{vol} = 1$ the metalimnion contributes more to the whole lake metabolically than it does volumetrically. Panel (**e**) shows the volumetric rate of NEP as a function of mean daily Z_{mix} : Z_{eu}. Each point represents one day, with a point only for days with at least one appropriate model fit in each depth-zone shown for plots (**a**–**d**). White, gray, and black points indicate oligotrophic, mesotrophic, and eutrophic lakes, respectively. Circles, squares/diamonds, and triangles represent monomictic, dimictic, and polymictic lakes, respectively. In plots (**c**, **d**) some outlying high points at Lake Ontario were excluded to aid interpretation.

Table 3. Results of principal components analysis (PCA). "Linear mixed models" rows show the results of linear mixed models that used the principal components as independent variables to explain metalimnetic contribution to whole-lake areal GPP and ER ($Prop_{metab}$). "β" indicates the estimated slope of the linear mixed model.

Principal component	PC1	PC2
% variation explained	36	32
Axis rotation		
Metalimnetic $Prop_{vol}$	−0.52	−0.42
Mean metalimnetic log PAR_z	−0.26	−0.65
Mean metalimnetic layer temperature	−0.68	0.19
Mean metalimnetic buoyancy frequency (N^2)	−0.43	0.60
Linear mixed models		
$Prop_{metab}$ for GPP	$\beta = -0.11 \pm 0.01$	$\beta = -0.02 \pm 0.02$
	$p < 0.001$, $R^2 = 0.26$	$p = 0.200$, $R^2 = 0.08$
$Prop_{metab}$ for ER	$\beta = -0.07 \pm 0.02$	$\beta = -0.10 \pm 0.02$
	$p < 0.001$, $R^2 = 0.09$	$p < 0.001$, $R^2 = 0.15$

estimates. However, within the metalimnion we found no evidence that mixing regime or local stability was associated with model convergence or fit metrics (Fig. 2; Supporting Information Fig. S4). Combined with previous sensitivity analyses (Obrador et al. 2014), we show that daily estimates of metabolic rates are robust to uncertainties in vertical diffusive fluxes (D_v) under many circumstances. However, there were exceptions, specifically in the deeper layers of polymictic Lake Müggel, which was often weakly stratified. The increased sensitivity at depth was likely due to the higher relative contribution of D_v and D_z to DO fluxes and the corresponding decrease in biological signal (Supporting Information Figs. S7–S16). Outside the case of the polymictic lake, it does not appear that the accuracy of estimated diffusive fluxes was an important factor in our reduced ability to describe diel variation in DO with the depth-integrated model below the upper mixed layer. This conclusion was supported by better model fits in the epilimnion where total diffusive fluxes (including D_s) contributed strongly to DO dynamics.

There are a range of physical processes that are unaccounted for by the depth-integrated framework, such as horizontal advection, metalimnetic intrusions, and internal seiches caused by wind forcing (Van de Bogert et al. 2007; Solomon et al. 2013). These processes introduce water masses into the metalimnion that are influenced by heterogeneous chemical conditions and biological communities (Van de Bogert et al. 2007, 2012; Solomon et al. 2013). For example, Sadro et al. (2011*a*) found that pelagic metabolic rates were commonly influenced by littoral habitats due to advection and changes in water-column stability. Combined with the sensitivity analyses, the patterns in model fits found among the depth zones in our study suggest that physical process errors were a considerable issue in the meta- and hypolimnion (Fig. 2). As physical processes are a function of lake morphology, we expected the degree of uncertainty in model estimates to vary among lakes according to size. However, we did not observe any consistent trends in measures of model fit across the gradient of lake areas (Supporting Information Fig. S5), suggesting process errors did not systematically bias our interpretations. Physical processes may have contributed to the high day-to-day variability in metabolic estimates because we found little evidence that this temporal variability was correlated with changes in light availability. Conversely, high day-to-day variability was typical even of epilimnetic rates that are estimated with higher certainty (Solomon et al. 2013; current study). Furthermore, selecting models with either adequate or poor fit did not influence the degree of among-day variability or vertical patterns in metabolism (Supporting Information Fig. S3). This suggests either that R^2 was a poor predictor of the importance of process errors, or that process errors did not contribute highly to among-day variability.

Quantifying the effect of physical processes on metabolic estimates using free-water measurements remains a considerable challenge and a priority for future research. It is crucial that ecological inferences made using the free-water method be interpreted in the context of physical processes (Sadro et al. 2011*a*) and estimate uncertainty (Cremona et al. 2014), especially below the upper mixed layer. We employed a number of methods to minimize the effect of process errors and assist in retrieving useful information on metabolic processes in deeper layers. These included temporal smoothing of time series and the calculation of thermal stratification and diffusive fluxes on sub-daily timescales (Coloso et al. 2011). Some confidence in the success of these procedures can be taken from the congruence between vertical patterns in metabolism and depth-integrated measures of Chl-*a* concentration where they were available (Supporting

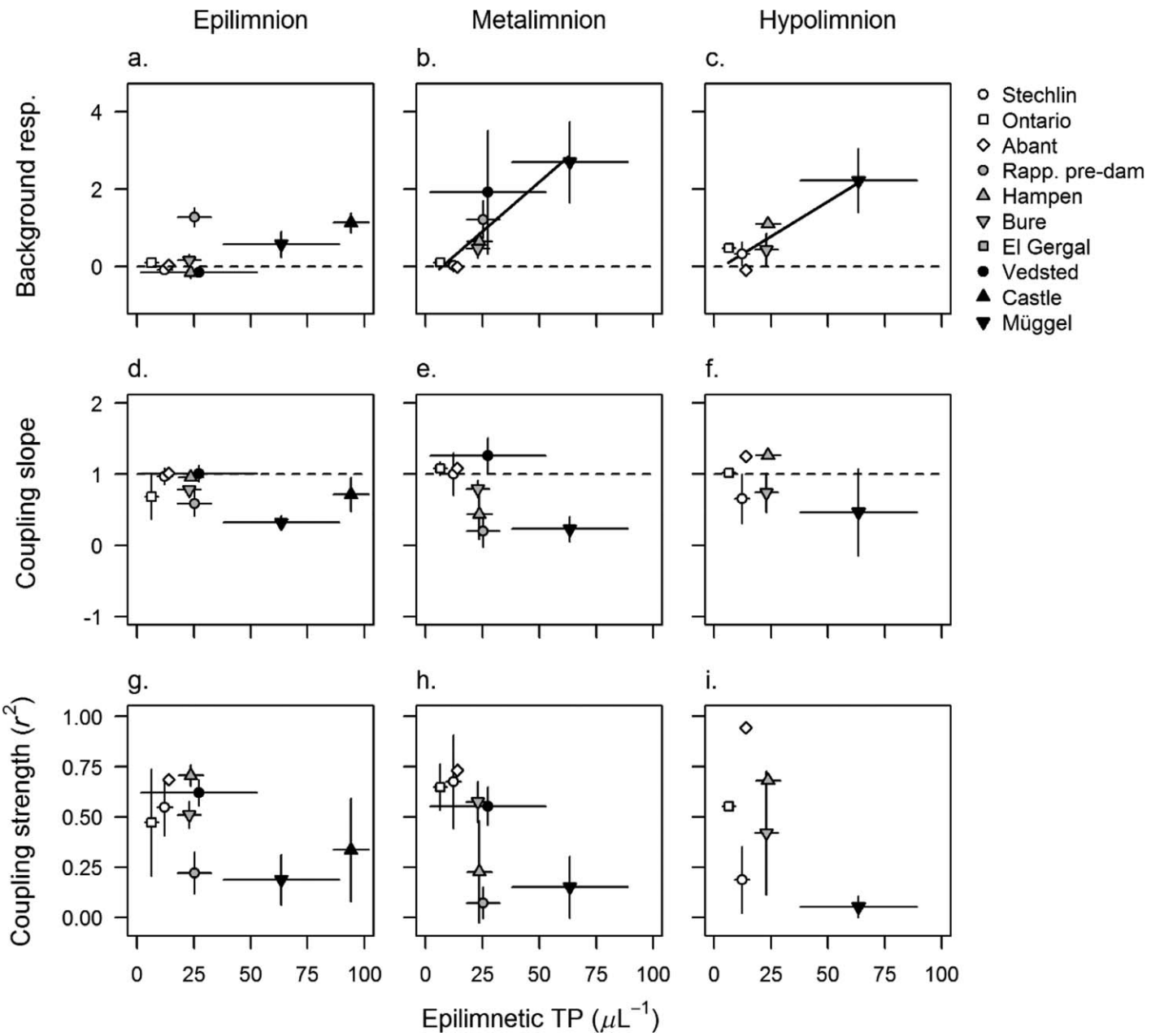

Fig. 5. Scatterplots of the correlation between nutrient concentration and the results of ER_{20}-to-GPP_{20} coupling relationships in the epi- (left; **a,d,g**), meta- (center; **b,e,h**), and hypolimnion (right; **c,f,i**). The top row shows the effect of mean (± SD) epilimnetic TP on mean (± SD) background respiration (i.e., intercept of correlation; mg O_2 L^{-1} d^{-1}) in all depth zones. The dashed horizontal line indicates a background respiration of zero (conceptually where there is no ER independent of GPP). The solid black lines show significant relationships in LMMs. The center row shows the relationship of epilimnetic TP with coupling slope (mg O_2 L^{-1} d^{-1}), with the dashed line at a slope of unity (representing a unit increase in ER for each unit increase in GPP). The bottom row shows the correction of mean TP with coupling strength (r^2). White, gray, and black points indicate oligotrophic, mesotrophic, and eutrophic lakes, respectively. Circles, squares/diamonds, and triangles represent monomictic, dimictic, and polymictic lakes, respectively.

Information Table S1). In our study, the vertical resolution of measurements did not affect metabolic estimate certainty, but maintaining a high resolution will increase the accuracy of temperature profiles and stratification patterns. This is important for calculating the contribution of specific lake zones, because the metalimnetic contribution is obviously sensitive to its thickness (Supporting Information Text 2 and Supporting Information Table S2). A high vertical resolution will also assist in cases such as Castle Lake where the development of hypolimnetic hypoxia (Supporting Information Fig. S9) could produce unrealistically sharp diffusive gradients if too few sensors are used.

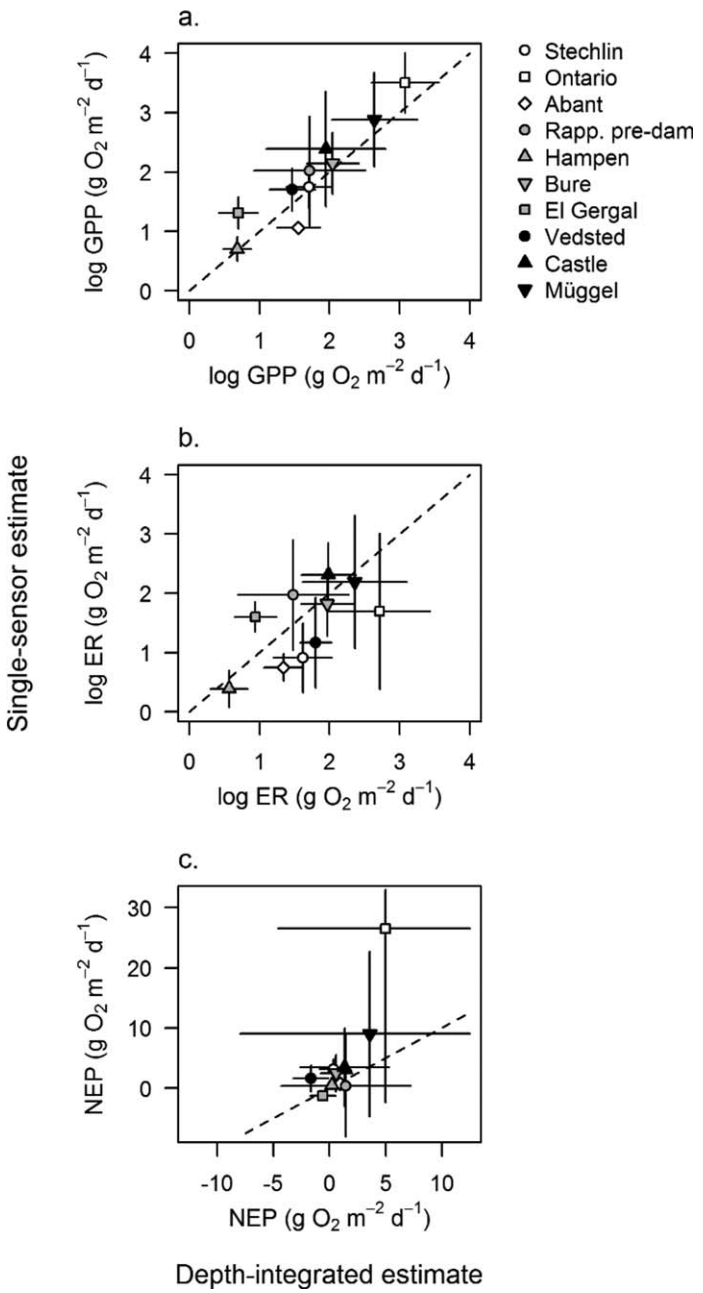

Fig. 6. Comparison of mean (± SD) areal whole-lake volume weighted (WLVW) metabolism calculated using the depth-integrated and single-sensor approaches for (**a**) GPP, (**b**) ER, and (**c**) NEP. The dashed line indicates the 1 : 1 relationship. White, gray, and black points indicate oligotrophic, mesotrophic, and eutrophic lakes, respectively. Circles, squares/diamonds, and triangles represent monomictic, dimictic, and polymictic lakes, respectively.

Vertical patterns in the efficiency of light utilization and metabolic coupling

An increase in light utilization efficiency explained cases of higher GPP rates in the metalimnion compared to the epilimnion despite the lower light availability. However, the mechanisms responsible for this pattern may vary among lakes. Depth-integrated measures of Chl-*a* concentration from a subset of lakes showed that increases in metalimnetic photosynthetic efficiency at Lakes Hampen, Vedsted, Castle (Obrador et al. 2014) and El Gergal (Table 2) were not caused by higher algal biomass in the metalimnion. This suggests that the phytoplankton communities in deeper layers were physiologically acclimated to the low-light conditions or benefited from the potentially higher nutrient availability and lower temperatures that reduce metabolic costs. In other lakes, such as oligotrophic Lakes Abant and Stechlin, and mesotrophic Lake Bure, Chl-*a* concentration peaked in the metalimnion. Deep chlorophyll maxima (DCM) are a common occurrence in many lakes (e.g., Hamilton et al. 2010; Brentrup et al. 2016), and their development will have a strong impact on vertical patterns of metabolism and metabolic coupling. Photosynthetic efficiency may also reflect the physiology of the species comprising the phytoplankton community. Rates of GPP and ER above Z_{eu} were conspicuously low at El Gergal for a mesotrophic system, potentially attributable to the dominance by a large, inefficient and slow-growing cyanobacterium (*Aphanizomenon flos-aquae*; Moreno-Ostos et al. 2016).

Our estimates corroborate previous findings that heterotrophic to balanced conditions generally prevail in the metalimnion (e.g., Sadro et al. 2011*a*), even when it was presumably well lit (Fig. 4e). This has been previously ascribed to ER being less depth-dependent than GPP (Coloso et al. 2008). However, vertical patterns in ER were similar to GPP in many lakes, at both in situ temperature and when standardized to 20°C (Fig. 1, Supporting Information S2). Days of autotrophy in the metalimnion of lakes from all trophic states and mixing regimes interspersed the predominant state of heterotrophy (Wilkinson et al. 2015). Despite high variability in GPP and ER rates among sites, metalimnetic NEP was relatively stable, with a mean of -0.08 ± 0.26 mg O_2 L^{-1} d^{-1} among lakes when excluding polymictic Lake Müggel, which displayed outstandingly high autotrophy in the metalimnion (Fig. 1). This relative stability was likely due to the metalimnetic ER_{20}-to-GPP_{20} coupling gradient being close to 1 in many lakes (Fig. 5e). Substrate limitation of heterotrophs is hypothesized to drive strong metabolic coupling (Sadro et al. 2011*b*; Solomon et al. 2013), and may be pronounced at depth because the OM in deeper layers typically contains a greater proportion of recalcitrant molecules with low biodegradability (Ostrom et al. 1998). A small number of mean coupling slope estimates > 1 were observed in the meta- and hypolimnion (Fig. 5e,f), suggesting greater than unit increases in ER for each unit increase in GPP. Priming of recalcitrant OM (Guenet et al. 2010) could produce such a pattern but evidence for this process in freshwater systems is inconclusive (Catalán et al. 2015). As these high slope estimates all occurred at low GPP it is more likely

that these estimates were artificially inflated by statistically influential data points with low GPP relative to ER.

Elevated background respiration in the meta- and hypolimnion of some mesotrophic and eutrophic sites suggests respiration of OM that was not recently or locally produced (Solomon et al. 2013). The metalimnion may be a zone with high degradation of particles that accumulate near the thermocline through a number of co-occurring mechanisms (Staehr et al. 2012*b*). This includes recently produced organic material sinking from the epilimnion, combined with large pools of recalcitrant dissolved organic matter (DOM). Particles such as zooplankton carcasses may be highly available in the metalimnion because they have higher residence times in stratified water columns and move slowly through the thermocline (Kirillin et al. 2012). Particulate organic matter (POM) accumulating below the mixed layer could also originate from resuspension of benthic material by internal seiches during stratification (Weyhenmeyer 1996) or external stream- and groundwater inputs that do not mix with the epilimnion. Higher nutrient availability below the epilimnion may also facilitate greater decomposition rates. For persisting heterotrophic conditions, there must be a net subsidy of carbon to the metalimnion and hypolimnion. In addition to accumulating particles, diel vertical migrations could play a role in linking surface and deeper waters, which has been relatively unexplored compared to physical mechanisms. Daily rates of microbial background respiration in the metalimnion could be spatially subsidized by zooplankton that migrate to surface waters at night and return to excrete epilimnion-derived DOM and POM in deeper layers (Watras et al. 2015). Furthermore, some motile autotrophs and mixotrophs vertically migrate to the surface to photosynthesize during the day (Salonen et al. 1984), and so respire carbon in deeper waters that was fixed in the surface waters.

Drivers of metalimnetic contribution to whole-lake metabolism

Contrary to expectations, light conditions in the metalimnion, as measured by the relation between mixing depth and photic zone ($Z_{mix} : Z_{eu}$), did not explain a large portion of the variation in metalimnetic $Prop_{metab}$ or $Prop_{metab} : Prop_{vol}$ alone (Fig. 4). Instead, our results suggested a collinear combination of physical and chemical variables, including light, nutrient concentration, temperature, water-column stability and metalimnetic volume drives metalimnetic $Prop_{metab}$ (Figs. 3, 4; Table 3). We did not find a strong association between mixing regime and metalimnetic $Prop_{metab}$, but the contribution will naturally be more temporally dynamic in polymictic lakes that have interspersed periods of mixed water columns. Concentration of TP in the epilimnion was negatively correlated with metalimnetic $Prop_{metab} : Prop_{vol}$, likely due to stimulating epilimnetic production that shades metalimnetic organisms (e.g., Laas et al. 2012). However, trends for GPP were highly influenced by the most eutrophic lakes, so that additional lakes are required to confirm these patterns. Despite the decreasing metalimnetic $Prop_{metab}$, absolute rates in the metalimnion increased slowly with TP concentration, until a threshold where the metalimnion became shaded (Castle Lake; Fig. 3a,b). These results imply that eutrophication of lake ecosystems may shift primary production from the metalimnion to the epilimnion, as observed for coastal systems (Lyngsgaard et al. 2014).

The variability in metalimnetic contribution to whole-lake metabolism was highly evident in the range of 0.5–1.0 $Z_{mix} : Z_{eu}$ (Fig. 4). While temporally interpolating K_D could introduce error, such variability was evident even at sites with sub-daily determination of K_D (e.g., Lake Stechlin). The dynamic nature of metalimnetic volume on both daily and seasonal bases (Coloso et al. 2011) is likely to affect its contribution to the depth-integrated areal rates (Staehr et al. 2012*b*). Fluctuations in thermal structure represent not only shifts in light availability, but also potentially important fluxes of OM, nutrients and biota among layers or between sediments and the water column. These fluxes may partly account for the high variability in metabolic estimates at polymictic Lake Müggel, where the longest run of consecutive stratified days was seven. In addition, mixing caused by wind or rain might stimulate metabolism by providing a nutrient or OM subsidy (Johengen et al. 2008; Giling et al. 2016), or depress GPP by suspending OM (Tsai et al. 2008; Sadro and Melack 2012). A key priority to further understand the chemical and physical drivers of variability in the metabolism of stratified lakes is obtaining a greater vertical and temporal resolution of data on nutrient concentration and OM composition (e.g., Wilkinson et al. 2014; Watras et al. 2015).

In conclusion, we found that the metalimnion can contribute substantially to whole-lake metabolism in many lakes using a depth-integrated approach. However, high variability in rates and collinearity among predictors meant that generalizations about the widespread importance of the metalimnion to water-column processes could not be made with broad lake categories such as trophic status, except for hypereutrophic lakes. Single sensors placed in the epilimnion retain value, especially for investigating the drivers of day-to-day variation in long term records due to high reliability of estimates and relative freedom from process errors that limit the accuracy of metabolic estimates in deeper layers. However, single-sensor estimates may not necessarily reflect whole-lake functioning; and deviate systematically from depth-integrated estimates of GPP. Overall, a depth-integrated approach enables enhanced understanding of how physical and biogeochemical processes influence the functioning of lake ecosystems as a whole.

References

Batt, R. D., and S. R. Carpenter. 2012. Free-water lake metabolism: Addressing noisy time series with a Kalman filter.

Limnol. Oceanogr.: Methods **10**: 20–30. doi:10.4319/lom.2012.10.20

Benson, B. B., and J. D. Krause. 1984. The concentration and isotopic fraction of oxygen dissolved in freshwater and seawater in equilibrium with the atmosphere. Limnol. Oceanogr. **29**: 620–632. doi:10.4319/lo.1984.29.3.0620

Boegman, L., J. Imberger, G. N. Ivey, and J. P. Antenucci. 2003. High-frequency internal waves in large stratified lakes. Limnol. Oceanogr. **48**: 895–919. doi:10.4319/lo.2003.48.2.0895

Boehrer, B., and M. Schultze. 2008. Stratification of lakes. Rev. Geophys. **46**: RG2005. doi:10.1029/2006RG000210

Boehrer, B., and M. Schultze. 2010. Density stratification and stability. *In* G. E. Likens [ed.], Lake ecosystem ecology: A global perspective. Academic Press.

Bouffard, D., L. Boegman, J. D. Ackerman, R. Valipour, and Y. R. Rao. 2014. Near-inertial wave driven dissolved oxygen transfer through the thermocline of a large lake. J. Great Lakes Res. **40**: 300–307. doi:10.1016/j.jglr.2014.03.014

Brentrup, J. A., and others. 2016. The potential of high-frequency profiling to assess vertical and seasonal patterns of phytoplankton dynamics in lakes: An extension of the Plankton Ecology Group (PEG) model. Inland Waters **6**: 565–580. doi:10.5268/IW-6.4.890

Brooks, S. P., and A. Gelman. 1997. General methods for monitoring convergence of iterative simulations. J. Comput. Graph. Stat. **7**: 434–455. doi:10.1080/10618600.1998.10474787

Catalán, N., A. M. Kellerman, H. Peter, F. Carmona, and L. J. Tranvik. 2015. Absence of a priming effect on dissolved organic carbon degradation in lake water. Limnol. Oceanogr. **60**: 159–168. doi:10.1002/lno.10016

Cole, J. J., and N. F. Caraco. 1998. Atmospheric exchange of carbon dioxide in a low-wind oligotrophic lake measured by the addition of SF6. Limnol. Oceanogr. **43**: 647–656. doi:10.4319/lo.1998.43.4.0647

Cole, J., and others. 2007. Plumbing the global carbon cycle: Integrating inland waters into the terrestrial carbon budget. Ecosystems **10**: 172–185. doi:10.1007/s10021-006-9013-8

Coloso, J. J., J. J. Cole, P. C. Hanson, and M. L. Pace. 2008. Depth-integrated, continuous estimates of metabolism in a clear-water lake. Can. J. Fish Aquat. Sci. **65**: 712–722. doi:10.1139/f08-006

Coloso, J., J. Cole, and M. Pace. 2011. Short-term variation in thermal stratification complicates estimation of lake metabolism. Aquat. Sci. **73**: 305–315. doi:10.1007/s00027-010-0177-0

Cremona, F., A. Laas, P. Nõges, and T. Nõges. 2014. High-frequency data within a modeling framework: On the benefit of assessing uncertainties of lake metabolism. Ecol. Model. **294**: 27–35. doi:10.1016/j.ecolmodel.2014.09.013

Del Giorgio, P. A., and P.J.L.B. Williams. 2005. The global significance of respiration in aquatic ecosystems: From single cells to the biosphere. *In* P. A. del Giorgio and P.J.L.B. Williams [eds.], Respiration in aquatic ecosystems. Oxford Univ. Press.

Giling, D. P., and others. 2016. Thermocline deepening boosts ecosystem metabolism: Evidence from a large-scale lake enclosure experiment simulating a summer storm. Glob. Chang. Biol. doi:10.1111/gcb.13512

Grace, M. R., D. P. Giling, S. Hladyz, V. Caron, R. M. Thompson, and R. Mac Nally. 2015. Fast processing of diel oxygen curves: Estimating stream metabolism with BASE (BAyesian Single-station Estimation). Limnol. Oceanogr.: Methods **13**: 103–114. doi:10.1002/lom3.10011

Guenet, B., M. Danger, L. Abbadie, and G. Lacroix. 2010. Priming effect: Bridging the gap between terrestrial and aquatic ecology. Ecology **91**: 2850–2861. doi:10.1890/09-1968.1

Hamilton, D. P., K. R. O'Brien, M. A. Burford, J. D. Brookes, and C. G. McBride. 2010. Vertical distributions of chlorophyll in deep, warm monomictic lakes. Aquat. Sci. **72**: 295–307. doi:10.1007/s00027-010-0131-1

Hanson, P. C., S. R. Carpenter, N. Kimura, C. Wu, S. P. Cornelius, and T. K. Kratz. 2008. Evaluation of metabolism models for free-water dissolved oxygen methods in lakes. Limnol. Oceanogr.: Methods **6**: 454–465. doi:10.4319/lom.2008.6.454

Holtgrieve, G. W., D. E. Schindler, T. A. Branch, and Z. T. A'mar. 2010. Simultaneous quantification of aquatic ecosystem metabolism and reaeration using a Bayesian statistical model of oxygen dynamics. Limnol. Oceanogr. **55**: 1047–1063. doi:10.4319/lo.2010.55.3.1047

Hondzo, M., and H. G. Stefan. 1993. Lake water temperature simulation model. J. Hydraul. Eng. **119**: 1251–1273. doi:10.1061/(ASCE)0733-9429(1993)119:11(1251)

Johengen, T. H., B. A. Biddanda, and J. B. Cotner. 2008. Stimulation of Lake Michigan plankton metabolism by sediment resuspension and river runoff. J. Great Lakes Res. **34**: 213–227. doi:10.3394/0380-1330(2008)34[213:SOLMPM]2.0.CO;2

Kirillin, G., H. P. Grossart, and K. W. Tang. 2012. Modeling sinking rate of zooplankton carcasses: Effects of stratification and mixing. Limnol. Oceanogr. **57**: 881–894. doi:10.4319/lo.2012.57.3.0881

Kirk, J. T. 1994. Light and photosynthesis in aquatic ecosystems. Cambridge Univ. Press.

Laas, A., P. Nõges, T. Kõiv, and T. Nõges. 2012. High-frequency metabolism study in a large and shallow temperate lake reveals seasonal switching between net autotrophy and net heterotrophy. Hydrobiologia **694**: 57–74. doi:10.1007/s10750-012-1131-z

Lyngsgaard, M. M., S. Markager, and K. Richardson. 2014. Changes in the vertical distribution of primary production in response to land-based nitrogen loading. Limnol. Oceanogr. **59**: 1679–1690. doi:10.4319/lo.2014.59.5.1679

McCree, K. J. 1981. Photosynthetically active radiation. *In* O. L. Lang, P. Novel, B. Osmond, and H. Ziegler [eds.], Physiological plant ecology. Encyclopedia of plant physiology (new series). Springer-Verlag.

McNair, J. N., L. C. Gereaux, A. D. Weinke, M. R. Sesselmann, S. T. Kendall, and B. A. Biddanda. 2013. New methods for estimating components of lake metabolism based on free-water dissolved-oxygen dynamics. Ecol. Model. **263**: 251–263. doi:10.1016/j.ecolmodel.2013.05.010

Meinson, P., A. Idrizaj, P. Nõges, T. Nõges, and A. Laas. 2015. Continuous and high-frequency measurements in limnology: History, applications, and future challenges. Environ. Rev. **24**: 52–62. doi:10.1139/er-2015-0030

Moreno-Ostos, E., R. L. Palomino-Torres, C. Escot, and J. M. Blanco. 2016. Planktonic metabolism in a Mediterranean reservoir during a near-surface cyanobacterial bloom. Limnetica **35**: 117–130.

Obrador, B., P. A. Staehr, and J. P. C. Christensen. 2014. Vertical patterns of metabolism in three contrasting stratified lakes. Limnol. Oceanogr. **59**: 1228–1240. doi:10.4319/lo.2014.59.4.1228

Odum, H. T. 1956. Primary production in flowing waters. Limnol. Oceanogr. **1**: 102–117. doi:10.4319/lo.1956.1.2.0102

Ostrom, N. E., D. T. Long, E. M. Bell, and T. Beals. 1998. The origin and cycling of particulate and sedimentary organic matter and nitrate in Lake Superior. Chem. Geol. **152**: 13–28. doi:10.1016/S0009-2541(98)00093-X

Plummer, M. 2003. JAGS: A program for analysis of Bayesian graphical models using Gibbs sampling. Proceedings of the 3rd International Workshop on Distributed Statistical Computing (DSC 2003).

Poole, H. H., and W. R. G. Atkins. 1929. Photoelectric measurements of submarine illumination throughout the year. J. Mar. Biol. Assoc. UK **16**: 297–324. doi:10.1017/S0025315400029829

R Development Core Team. 2014. R: A language and environment for statistical computing. R Foundation for Statistical Computing, Vienna, Austria. ISBN 3-900051-07-0. Available from http://www.R-project.org

Read, J. S., D. P. Hamilton, I. D. Jones, K. Muraoka, L. A. Winslow, R. Kroiss, C. H. Wu, and E. Gaiser. 2011. Derivation of lake mixing and stratification indices from high-resolution lake buoy data. Environ. Model. Softw. **26**: 1325–1336. doi:10.1016/j.envsoft.2011.05.006

Rimmer, A., Y. Aota, M. Kumagai, and W. Eckert. 2005. Chemical stratification in thermally stratified lakes: A chloride mass balance model. Limnol. Oceanogr. **50**: 147–157. doi:10.4319/lo.2005.50.1.0147

Rose, K. C., L. A. Winslow, J. S. Read, E. K. Read, C. T. Solomon, R. Adrian, and P. C. Hanson. 2014. Improving the precision of lake ecosystem metabolism estimates by identifying predictors of model uncertainty. Limnol. Oceanogr.: Methods **12**: 303–312. doi:10.4319/lom.2014.12.303

Sadro, S., J. M. Melack, and S. Macintyre. 2011*a*. Depth-integrated estimates of ecosystem metabolism in a high-elevation lake (Emerald Lake, Sierra Nevada, California). Limnol. Oceanogr. **56**: 1764–1780. doi:10.4319/lo.2011.56.5.1764

Sadro, S., C. E. Nelson, and J. M. Melack. 2011*b*. Linking diel patterns in community respiration to bacterioplankton in an oligotrophic high-elevation lake. Limnol. Oceanogr. **56**: 540–550. doi:10.4319/lo.2011.56.2.0540

Sadro, S., and J. Melack. 2012. The effect of an extreme rain event on the biogeochemistry and ecosystem metabolism of an oligotrophic high-elevation lake. Arct. Antarct. Alp. Res. **44**: 222–231. doi:10.1657/1938-4246-44.2.222

Sadro, S., G. W. Holtgrieve, C. T. Solomon, and G. R. Koch. 2014. Widespread variability in overnight patterns of ecosystem respiration linked to gradients in dissolved organic matter, residence time, and productivity in a global set of lakes. Limnol. Oceanogr. **59**: 1666–1678. doi:10.4319/lo.2014.59.5.1666

Salonen, K., R. I. Jones, and L. Arvola. 1984. Hypolimnetic phosphorus retrieval by diel vertical migrations of lake phytoplankton. Freshw. Biol. **14**: 431–438. doi:10.1111/j.1365-2427.1984.tb00165.x

Solomon, C. T., and others. 2013. Ecosystem respiration: Drivers of daily variability and background respiration in lakes around the globe. Limnol. Oceanogr. **58**: 849–866. doi:10.4319/lo.2013.58.3.0849

Song, C., W. K. Dodds, M. T. Trentman, J. Rüegg, and F. Ballantyne. 2016. Methods of approximation influence aquatic ecosystem metabolism estimates. Limnol. Oceanogr.: Methods **14**: 557–569. doi:10.1002/lom3.10112

Staehr, P. A., D. Bade, M. C. Van de Bogert, G. R. Koch, C. Williamson, P. Hanson, J. J. Cole, and T. Kratz. 2010. Lake metabolism and the diel oxygen technique: State of the science. Limnol. Oceanogr.: Methods **8**: 628–644. doi:10.4319/lom.2010.8.0628

Staehr, P., J. Testa, W. Kemp, J. Cole, K. Sand-Jensen, and S. Smith. 2012*a*. The metabolism of aquatic ecosystems: History, applications, and future challenges. Aquat. Sci. **74**: 15–29. doi:10.1007/s00027-011-0199-2

Staehr, P. A., J. P. A. Christensen, R. D. Batt, and J. S. Read. 2012*b*. Ecosystem metabolism in a stratified lake. Limnol. Oceanogr. **57**: 1317–1330. doi:10.4319/lo.2012.57.5.1317

Sweers, H. E. 1970. Vertical diffusivity coefficient in a thermocline. Limnol. Oceanogr. **15**: 273–280. doi:10.4319/lo.1970.15.2.0273

Tsai, J. W., and others. 2008. Seasonal dynamics, typhoons and the regulation of lake metabolism in a subtropical humic lake. Freshw. Biol. **53**: 1929–1941. doi:10.1111/j.1365-2427.2008.02017.x

Van de Bogert, M. C., S. R. Carpenter, J. J. Cole, and M. L. Pace. 2007. Assessing pelagic and benthic metabolism using free water measurements. Limnol. Oceanogr.: Methods **5**: 145–155. doi:10.4319/lom.2007.5.145

Van de Bogert, M. C., D. L. Bade, S. R. Carpenter, J. J. Cole, M. L. Pace, P. C. Hanson, and O. C. Langman. 2012. Spatial heterogeneity strongly affects estimates of ecosystem metabolism in two north temperate lakes. Limnol. Oceanogr. **57**: 1689–1700. doi:10.4319/lo.2012.57.6.1689

Watras, C. J., K. A. Morrison, J. T. Crawford, C. P. McDonald, S. K. Oliver, and P. C. Hanson. 2015. Diel

cycles in the fluorescence of dissolved organic matter in dystrophic Wisconsin seepage lakes: Implications for carbon turnover. Limnol. Oceanogr. **60**: 482–496. doi: 10.1002/lno.10026

Weyhenmeyer, G. A. 1996. The influence of stratification on the amount and distribution of different settling particles in Lake Erken. Can. J. Fish. Aquat. Sci. **53**: 1254–1262. doi:10.1139/cjfas-53-6-1254

Wilcock, R.J.J.W.N., G. B. McBride, K. J. Collier, B. T. Wilson, and B. A. Huser. 1998. Characterisation of lowland streams using a single-station diel curve analysis model with continuous monitoring data for dissolved oxygen. N. Z. J. Mar. Freshw. Res. **32**: 67–79. doi:10.1080/00288330.1998.9516806

Wilkinson, G. M., S. R. Carpenter, J. J. Cole, and M. L. Pace. 2014. Use of deep autochthonous resources by zooplankton: Results of a metalimnetic addition of ^{13}C to a small lake. Limnol. Oceanogr. **59**: 986–996. doi:10.4319/lo.2014.59.3.0986

Wilkinson, G. M., J. J. Cole, M. L. Pace, R. A. Johnson, and M. J. Kleinhans. 2015. Physical and biological contributions to metalimnetic oxygen maxima in lakes. Limnol. Oceanogr. **60**: 242–251. doi:10.1002/lno.10022

Acknowledgments

The collaboration was made possible by the activities of Networking Lake Observations in Europe (NETLAKE), funded by the European Corporation in Science and Technology (COST) action ES1201. Ideas for this manuscript were initiated at a NETLAKE workshop organized by PAS, BO and E. Jennings in Roskilde, Denmark. Acquisition of Lake Stechlin data was facilitated by grants from the German Federal Ministry of Education and Research (BMBF; no. 033L041B) and the German Research Foundation (DFG Core Facility; no. GE 1775/2-1) to M.O. Gessner, and from the Leibniz Association (project 'TemBi'; SAW-2011-IGB-2) to P. Casper and HPG. We thank S. A. Berger, C. Engelhardt, M.O. Gessner, M. Lentz, J. C. Nejstgaard and A. Penske for provision of ancillary data from Lake Stechlin. Data from Danish lakes were supported by the Danish Centre for Lake Restoration (CLEAR). Data collection from Lake Abant was funded by the Scientific and Technological Research Council of Turkey (TUBITAK) (Grant No: 111Y059). Data collection for El Gergal Reservoir was supported by EMASESA and projects EU-ENV/UK/000604 and CGL2005-04070. Lake Ontario data was provided by B. Weidel and M. Paufve and funding for data collection at Lake Ontario came from the Great Lakes Restoration Initiative, Great Lakes Fishery Commission, and New York State Department of Conservation. Two anonymous reviewers provided comments that greatly improved this manuscript.

Conflict of Interest

None declared.

Submitted 17 May 2016
Revised 16 November 2016
Accepted 02 December 2016

Associate editor: Marguerite Xenopoulos